OPEN

Correspondence and requests for materials should be addressed to J.-B.B. (jbosch@iconcologia.net); V.M. (vmicol@umh.es) or J. A.M. (jmenendez@iconcologia.net; jmenendez@idibgi.org)

* These authors contributed equally to this work.

Silibinin suppresses EMT-driven erlotinib resistance by reversing the high *miR-21/* low *miR-200c* signature *in vivo*

Sílvia Cufí[1,2]*, Rosa Bonavia[3]*, Alejandro Vazquez-Martin[1,2]*, Cristina Oliveras-Ferraros[1,2], Bruna Corominas-Faja[1,2], Elisabet Cuyàs[1,2], Begoña Martin-Castillo[2,5], Enrique Barrajón-Catalán[6,7], Joana Visa[3], Antonio Segura-Carretero[8], Jorge Joven[9], Joaquim Bosch-Barrera[2,4], Vicente Micol[6,7] & Javier A. Menendez[1,2]

[1]Metabolism & Cancer Group, Translational Research Laboratory, Catalan Institute of Oncology, Girona, Catalonia (Spain), [2]Girona Biomedical Research Institute (IDIBGi), Girona, Catalonia (Spain), [3]Animal Care Facility, IDIBELL, L'Hospitalet de Llobregat, Barcelona, Catalonia (Spain), [4]Medical Oncology, Catalan Institute of Oncology, Girona, Catalonia (Spain), [5]Unit of Clinical Research, Catalan Institute of Oncology, Girona, Catalonia (Spain), [6]Molecular and Cellular Biology Institute (IBMC), Miguel Hernández University, Elche, Alicante (Spain), [7]Monteloeder, Inc., Elche, Alicante (Spain), [8]Department of Analytical Chemistry, Faculty of Sciences, University of Granada, Granada, Spain, [9]Unitat de Recerca Biomèdica (URB-CRB), Institut d'Investigació Sanitaria Pere i Virgili (IISPV), Universitat Rovira i Virgili, Reus, Catalonia (Spain).

The flavolignan silibinin was studied for its ability to restore drug sensitivity to EGFR-mutant NSCLC xenografts with epithelial-to-mesenchymal transition (EMT)-driven resistance to erlotinib. As a single agent, silibinin significantly decreased the tumor volumes of erlotinib-refractory NSCLC xenografts by approximately 50%. Furthermore, the complete abrogation of tumor growth was observed with the co-treatment of erlotinib and silibinin. Silibinin fully reversed the EMT-related high *miR-21/*low *miR-200c* microRNA signature and repressed the mesenchymal markers *SNAIL, ZEB,* and *N-cadherin* observed in erlotinib-refractory tumors. Silibinin was sufficient to fully activate a reciprocal mesenchymal-to-epithelial transition (MET) in erlotinib-refractory cells and prevent the highly migratogenic phenotype of erlotinib-resistant NSCLC cells. Given that the various mechanisms of resistance to erlotinib result from EMT, regardless of the EGFR mutation status, a water-soluble, silibinin-rich milk thistle extract might be a suitable candidate therapy for upcoming clinical trials aimed at preventing or reversing NSCLC progression following erlotinib treatment.

The discovery of somatic activating mutations in the epidermal growth factor receptor (EGFR) kinase domain has radically altered the treatment options of patients with non-small cell lung cancer (NSCLC)[1–5]. For example, Caucasian patients harboring activating mutations in the EGFR kinase domain, such as a deletion in exon 19 or *L858R*, have shown significant responses to the EGFR tyrosine kinase inhibitor (TKI) erlotinib, including a 70% response rate, 14-month progression-free survival, and 27-month median survival. Accordingly, the EGFR TKIs erlotinib or gefitinib have become the standard of care for first-line treatment in patients with advanced NSCLC and whose tumors harbor activating mutations in the kinase domain of EGFR. However, despite the encouraging clinical findings showing a favorable response to first- and second-line EGFR TKIs, advanced NSCLC patients with EGFR mutations often respond unpredictably to initial EGFR TKI therapy. Additionally, patients who initially show dramatic responses invariably relapse due to the development of drug resistance. Intriguingly, some NSCLC patients with wild-type EGFR also benefit from treatments with EGFR TKIs. Not surprisingly, numerous research groups are attempting to identify more effective predictive biomarkers for assessing the response or resistance to EGFR TKIs to optimize therapy for individual patients.

The acquisition of resistance to EGFR TKIs has been attributed to two main mechanisms reviewed in [6–12]. The first is the emergence of malignant clones containing second-site mutations in the EGFR kinase domain that abrogate the inhibitory activity of EGFR TKIs. The most common lesion is the so-called "gatekeeper mutation", which involves a substitution of methionine for threonine at position 790 (*T790M*). The second well-known mechanism of resistance to gefitinib or erlotinib is the amplification of the *MET* receptor tyrosine kinase (RTK) gene, which activates downstream intracellular signaling independently of EGFR. *EGFR T790M* and *MET*

amplification account for approximately 60–70% of all known causes of acquired resistance to gefitinib or erlotinib; these amplifications are not mutually exclusive and can be detected in the same resistant tumor or may occur independently in different metastatic sites in the same patient. Consequently, ongoing research has been focused on identifying the molecular mechanisms accounting for the 30–40% of EGFR TKI-resistant, EGFR-mutant tumors that do not carry *EGFR* mutations or *MET* amplification[13]. In this regard, emerging evidence strongly suggests that the mesenchymal phenotype is closely related to the lack of responsiveness to EGFR TKIs[14–25]. First, although NSCLC cell lines with *EGFR*-activating mutations are the most sensitive to erlotinib, mesenchymal cell lines are highly resistant to erlotinib when compared to epithelial cell lines. Second, the correlation between an epithelial-to-mesenchymal transition (EMT) signature and greater resistance to erlotinib can be observed, even in *EGFR* wild-type gene cells exhibiting a mesenchymal-like phenotype. Third, genetic and histological analyses of tumor biopsies from NSCLC patients with acquired resistance to EGFR inhibitors have revealed that a subgroup of resistant carcinomas exhibit a pronounced EMT. Fourth, the activation of the receptor tyrosine kinase AXL, which confers acquired resistance to erlotinib in pre-clinical models of *EGFR*-mutated NSCLCs and is overexpressed in approximately 20% of post-erlotinib-treated patients with EGFR TKI resistance, has been associated with the development of an EMT phenotype. Fifth, in NSCLC, the EMT phenomenon does not appear to be a general marker of resistance toward commonly used chemotherapeutics, such as pemetrexed, docetaxel, and paclitaxel, as mesenchymal cells appear to be relatively more sensitive to cisplatin, gemcitabine, and vinorelbine. Sixth, an EMT signature that highlights the different patterns of drug responsiveness in epithelial and mesenchymal NSCLC cells has prognostic value for early-stage NSCLC and can also predict resistance to EGFR TKIs, regardless of the EGFR mutation status.

Emerging data have repeatedly implicated EMT in contributing to both innate and acquired resistance to erlotinib; accordingly, it might be tempting to suggest that EMT is a core resistance mechanism that might be targeted to bypass the inhibition of the EGFR pathway in NSCLC. Indeed, elucidating how EMT could be prevented or reversed in NSCLC should enable the development of new strategies aimed at optimizing the efficacy of EGFR TKIs to improve the therapeutic outcome of NSCLC patients. Although the inhibition of EMT can be a critical strategy for delaying or preventing tumor progression after treatment with EGFR TKIs, the reversal of the EMT-driven erlotinib-refractory phenotype is urgently needed to expand the current EMT-targeted therapies. In this regard, a landmark study showed that the combination of EGFR TKIs with the lignin silibinin, the bioactive constituent of silymarin isolated from the dried fruits of the milk thistle (*Silybum marianum*) plant[26–29], drastically suppressed tumor growth. This was the case for both primary tumors and the cells that had acquired TKI resistance *via* the *EGFR T790M* mutation[30]. This finding might open a new, unexpected therapeutic avenue for the clinical management of EMT-driven, acquired resistance to erlotinib. Silibinin, a potent natural agent, appears to reverse EMT by decreasing the levels of key EMT transcription factors, such as SLUG, and increasing the expression levels of E-cadherin[31–33]. Because the ability of silibinin to overcome the erlotinib resistance that is attributed to mechanisms other than second-site *EGFR* mutations has not been explored and given that the poor water solubility and low bioavailability of silibinin might severely limit its clinical efficacy in NSCLC patients, we decided to explore whether a milk thistle extract rich in silibinin-meglumine, a commercially used water-soluble form of silibinin complexed with the excipient amino-sugar meglumine (**Fig. 1**), can reverse acquired resistance to EGFR TKIs in animal models. Here, we present the first evidence that, in the absence of second-site *EGFR* mutations or the activation of MET or AXL, a water-soluble formulation of the flavolignan silibinin, efficiently circumvents EMT-driven resistance to erlotinib *via* a mechanism that involves, at least in part, the restoration of the imbalance of such EMT-related microRNAs as *miR-21* and *miR-200c* in erlotinib-refractory tumors *in vivo*.

Results

In the absence of second-site EGFR mutations, erlotinib-refractory, EGFR-mutant NSCLC mouse xenografts exhibit faster tumor growth than erlotinib-responsive xenografts. We subcutaneously implanted parental PC-9 cells and PC-9/Erl-R derivatives[34] in athymic nude mice to compare whether the acquisition of resistance to erlotinib significantly altered the tumor-forming ability of EGFR-mutant NSCLC cells. In the absence of erlotinib treatment, the PC-9/Erl-R cells exhibited significantly higher tumorigenicity than the parental PC-9 cells. The PC-9/Erl-R cells established larger tumors with shorter latencies in comparison to the parental PC-9 cells (**Supplementary Fig. 1**). To confirm the genetic changes, which were previously described in cultured parental and resistant cells *in vitro*[34], following the acquired resistance to erlotinib *in vivo*, we examined genomic DNA directly isolated from frozen tumors. We assessed the status of 85 possible mutations in the EGFR pathway using the Human EGFR Pathway qBiomarker Somatic Mutation PCR array, which combines allele-specific amplification and 5′-hydrolysis probe detection to detect as little as 0.01% somatic mutations in a background of wild-type genomic DNA. Similarly, we assessed the erlotinib-sensitizing deletion mutation *ΔE746-A750* in the parental PC-9 cells. However, we failed to detect new co-occurring mutations in the *EGFR* gene (including the gatekeeper EGFR-*T790M* mutation, in the tumors generated by the PC-9/Erl-R cells, which maintained the same expression level of EGFR *ΔE746-A750* as the PC-9 cells (**Supplementary Fig. 1**). By using Human *EGFR* Pathway qBiomarker Somatic Mutation PCR Arrays, we also confirmed that the PC-9/Erl-R tumors did not harbor any secondary mutations in the *KRAS*, *NRAS*, or *BRAF* genes (data not shown).

Oral administration of silibinin delays tumor progression in erlotinib-refractory EGFR-mutant NSCLC mouse xenografts. Silibinin is the primary active constituent of a crude extract (silymarin) from milk thistle plant (*Silybum marianum*) seeds. We explored the ability of an oral milk thistle extract formulation that was enriched (30% *w/w*) with a water-soluble form of silibinin complexed with the amino-sugar meglumine to inhibit the growth of a PC-9/Erl-R xenograft animal model. When the tumor volumes reached approximately 100 mm³, as measured with calipers, the mice were randomly allocated into groups of 6 animals each. The groups received erlotinib, silibinin, erlotinib and silibinin, or vehicles by oral gavage. The mice in each group were followed, and their tumors were measured during the 35 days of treatment; the tumor volume was calculated for each mouse at each time point. **Fig. 2A** shows the rate of tumor growth in the four treatment groups, with the data plotted as the mean tumor volume in each group over time. In the erlotinib-treated animals, the tumor volumes were larger than the initial volume at all time points, and this increase became statistically significant at day 14. When compared to the animals in the vehicle-treated group (mean tumor volumes of 965 ± 155 mm³), 5 weeks of treatment with erlotinib for 5 days/week at 100 mg/kg body weight by oral gavage failed to prevent tumor growth in animals xenografted with PC-9/Erl-R cells, showing a mean tumor volume was as high as 767 ± 180 mm³. However, 5 weeks of treatment with silibinin for 5 days/week at 100 mg/kg body weight by oral gavage caused a marked time-dependent reduction in xenograft growth. Thus, compared to the mean xenograft tumor volume in both the untreated control and erlotinib-treated animals, the mean tumor volume of the silibinin-treated mice was significantly smaller (460 ± 120 mm³). Throughout the duration of the experiment, the mice
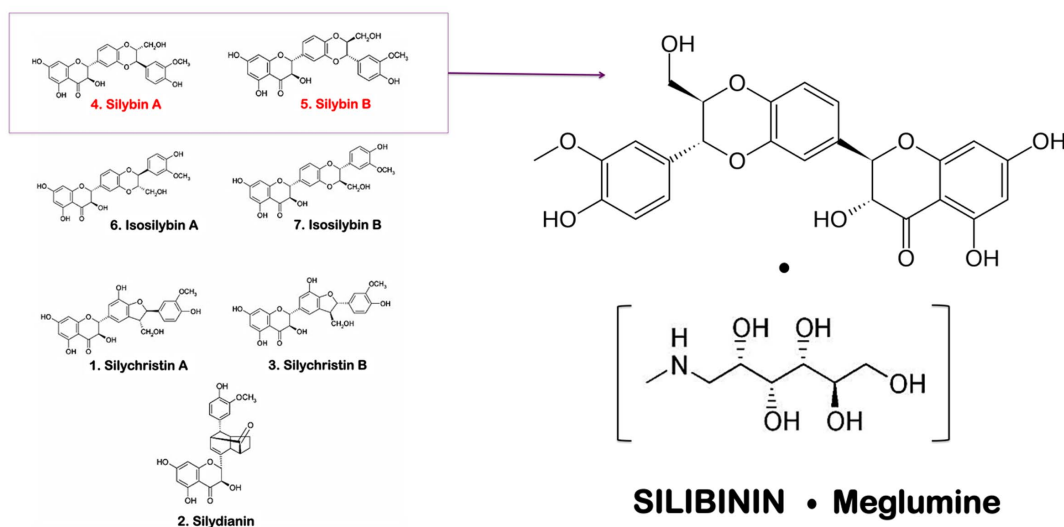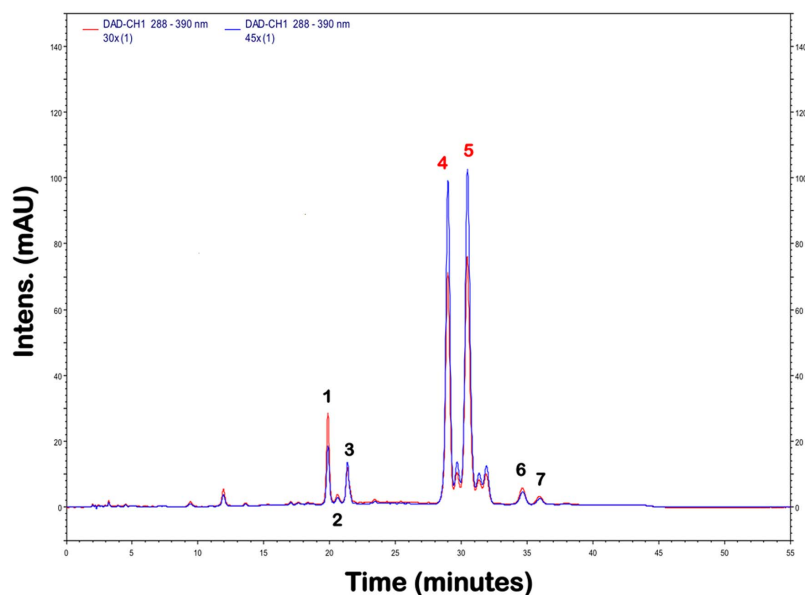
Figure 1 | HPLC chromatogram of milk thistle extract with 30% (*w/w*) of water-soluble silibinin meglumine at 288 nm. Compounds are identified by number as follows: silychristin A (1), silydianin (2), silychristin B (3), silybin A (4), silybin B (5), isosilybin A (6) and isosilybin B (7). Chemical structures of the compounds are also shown.

treated with silibinin did not show any gross signs of toxicity or possible adverse effects, as assessed by body weight gain and diet consumption profiles (data not shown). Taken together, these results demonstrate the *in vivo* antitumor efficacy of oral silibinin administration on erlotinib-refractory, EGFR-mutant tumor xenografts, without any apparent signs of toxicity.

Systemic silibinin administration sensitizes erlotinib-resistant xenografts to erlotinib. Daily oral gavage of the mice with erlotinib-treated xenografts with silibinin resulted in a dramatic reduction in the mean tumor volume to 143 ± 60 mm³. Although erlotinib treatment only reduced the tumor volume of the PC-9/Erl-R xenografts by 20% at 35 days post-treatment, the combined treatment of erlotinib and silibinin reduced the tumor volume of the PC-9/Erl-R xenografts by an impressive 85% over the same treatment period. Thus, although the tumors increased to 7 times their initial volume in the group treated with erlotinib, there were no

statistically significant changes in tumor size over the same time period in the erlotinib and silibinin-treated mice. These findings strongly suggest that the erlotinib-refractory PC-9/Erl-R xenografts were sensitized to the tumor growth inhibitory effects of erlotinib in the presence of silibinin. This was reflected by the percentage of tumor growth inhibition, which was calculated as 1-treated/control volume ratios (1-T/C) (**Fig. 2B**). The inhibitory effect of erlotinib was modest, reaching a maximum after 4 weeks (26%) and decreasing toward the end of the treatment to the very low levels of activity achieved during the first weeks of treatment (10%–20%). Conversely, after 2 weeks of treatment, the anti-tumor activity of the single agent silibinin was equivalent to the highest inhibitory effect (24%) of erlotinib, which was achieved after 4 weeks of treatment. The anti-tumor effect of silibinin reached a maximum after 4 weeks (52%) and remained constant until the end of the 5-week treatment schedule (52%). Of note, the anti-tumor activity in the combined erlotinib and silibinin group (57%) was already greater
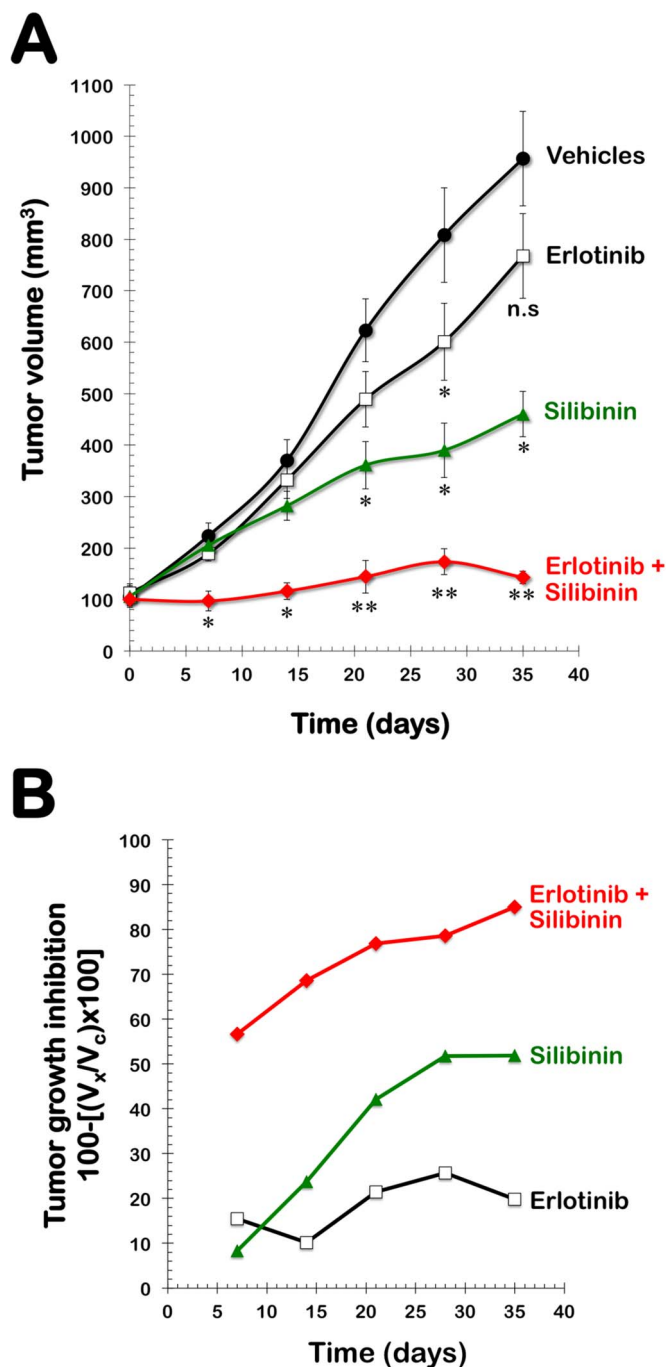
Figure 2 | Oral treatment of erlotinib-refractory, EGFR-mutant NSCLC xenograft-bearing animals with silibinin: Impact on the efficacy of the EGFR TKI erlotinib *in vivo*. (A). Shown are the mean tumor volumes (±SD) in PC-9/Erl-R xenograft-bearing nude mice following oral gavage with erlotinib, silibinin or erlotinib *plus* silibinin for five weeks. Data represent means ± SD. *$P < 0.05$ (Student's t-test), **$P < 0.005$ (Student's t-test), and n.s. non-statistically significant results (Student's t-test), *versus* erlotinib-treated mice. (B). Antitumor activity was calculated for individual tumors as the percentage of tumor growth inhibition, according to the following formula: $100 - [(V_x/V_c) \times 100]$, where V_x is the tumor volume for treated mice and V_c is the tumor volume in the control group at a given x time.

after only 7 days of treatment than the maximum activity achieved at any time with the single-agent treatment. Moreover, the inhibitory effect of the combination increased in a time-dependent manner, reaching a maximum of 85% after 35 days.

Oral silibinin reduces the expression of EMT-related markers in erlotinib-refractory tumors *in vivo*. MicroRNAs (miRNAs) are single-stranded, 19 to 25-nucleotide-long, short RNAs that elicit regulatory effects on the post-transcriptional regulation of genes by binding to the 3′ untranslated region (3′UTR) of a target messenger RNA (mRNA), leading to translational repression or target mRNA cleavage. It is well established that miRNAs regulate EMT through the regulation of E-cadherin and other molecules, such as the transcription factor ZEB[35–40]. Additionally, recent studies have suggested that natural agents, including the polyphenols curcumin, (-)-epigallocatechin-3-gallate, and resveratrol, can alter miRNA expression profiles, leading to the reversal of EMT and enhancing the efficacy of conventional cancer therapeutics[41–50]. As such, we hypothesized that the plant polyphenol silibinin may also function as a previously unrecognized regulator of miRNAs that might lead to the reversal of the EMT phenotype. After 35 days of oral treatment with silibinin, tumors were collected and snap frozen for the isolation of total RNA. We then used a customized array for the quantitative, real-time PCR (qRT-PCR) analysis of 12 miRNAs that are functionally associated with EMT and the reciprocal mesenchymal-to-epithelial transition (MET), namely *miR-31*, *miR-21*, *miR-10b*, *miR-103*, *miR-9*, *let-7a*, *miR-200a*, *miR-205*, *miR-200c*, *miR-141*, *miR-155*, and *miR-429*. Using a cutoff of a 4-fold or greater difference to determine significant regulatory effects on miRNA expression levels, we found that the expression of EMT-driving *miR-21*[51–56] was drastically augmented in the PC-9/Erl-R-derived tumor tissues (15 ± 3-fold up-regulation; **Fig. 3**). *miR-31*, another oncogenic miRNA that is closely related to the pro-EMT effects of *miR-21*[51,57–59], was also found to be significantly overexpressed in the PC-9/Erl-R-derived tumor tissues (5.7 ± 1-fold up-regulation; **Fig. 3**). Conversely, *miR-200c*, a member of the miR-200 family and a key regulator of EMT that controls the transition between non-stem cell-like and cancer stem cell (CSC)-like cellular states and that has been shown to determine the response to EGFR TKIs[37,41,60–64], was found to be significantly underexpressed in the PC-9/Erl-R-derived tumor tissues (−3.4 ± 1-fold down-regulation; **Fig. 3**). Remarkably, the PC-9/Erl-R tumor samples treated with oral silibinin exhibited a full reversion of the respective up- or down-regulation of *miR-21*, *miR-31*, and *miR-200c* that was observed in the erlotinib-refractory PC-9/Erl-R tumors. Thus, the systemic administration of silibinin was able to restore the altered expression pattern of EMT-related miRNAs, returning them to the control levels observed in the erlotinib-responsive PC-9 parental tumors (**Fig. 3**).

Recent studies have revealed that *miR-21* expression confers tumor aggressiveness and metastatic potential, at least in part, by inducing the expression of and cooperating with the EMT master regulatory gene, *SNAIL1*[55]. Accordingly, we used qRT-PCR to explore whether the ability of silibinin to down-regulate *miR-21* expression affected the expression of *SNAIL1*. We confirmed that *SNAIL1* expression was markedly reduced in the tumor tissues harvested from the erlotinib-refractory PC-9/Erl-R xenografts and that silibinin treatment restored *SNAIL1* expression to the basal levels observed in the erlotinib-responsive PC-9-formed xenograft tissues (**Fig. 3**). Because all the studies published to date have described the epithelial transcriptional repressors *ZEB1* and *ZEB2* as critical targets of *miR-200* family members, we examined whether the ability of silibinin to promote the re-expression of *miR-200c* significantly impacted the expression of its predicted targets, *ZEB1/2*. qRT-PCR analyses confirmed that the *ZEB1* gene was significantly up-regulated in the erlotinib-refractory PC-9/Erl-R xenograft tissues (**Fig. 3**). In contrast, oral treatment with silibinin down-regulated *ZEB1* gene expression to the basal levels observed in the erlotinib-responsive PC-9 xenograft tissues. These results suggested that the antagonism of *miR-21* and re-expression of *miR-200c* induced by silibinin decreased the mRNA expression of mesenchymal phenotype cell
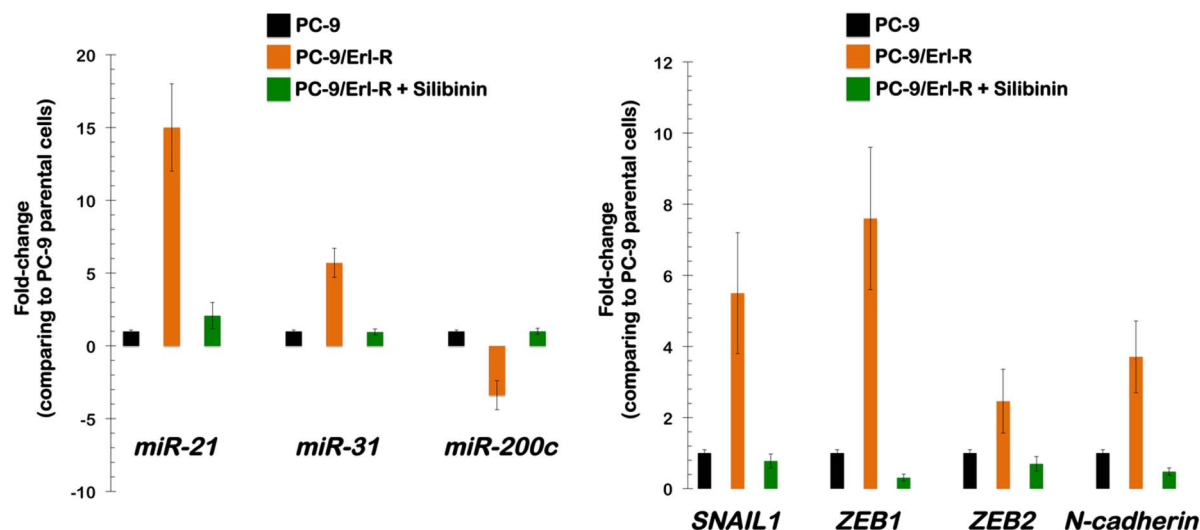
4

Figure 3 | Oral treatment with silibinin reverses the EMT-related high *miR-21*/low *miR200c* microRNA signature and downregulates mesenchymal markers in erlotinib-refractory EGFR-mutant NSCLC xenograft-bearing animals. Figure shows the difference (fold-change mean values ± SD *versus* untreated PC-9 parental cells; n = 4) in the three differentially expressed miRNAs (*i.e.,* *miR-21*, *miR-31*, and *miR-200c*) between erlotinib-resistant PC-9/Erl-R tumor samples and erlotinib-responsive PC-9 tumor samples following oral treatment with silibinin for five weeks (*left panel*). Figure also shows the effects of oral treatment with silibinin in the expression of the mesenchymal markers *SNAIL1*, *ZEB1*, *ZEB2*, and *N-cadherin* (fold-change mean values ± SD *versus* untreated PC-9 parental cells; n = 4), which were found significantly overrepresented in erlotinib-refractory EGFR-mutant NSCLC xenografts (*right panel*).

biomarkers. We also studied the relative mRNA expression of *N-cadherin* (*CDH2*), a mesenchymal cadherin associated with EMT that has consistently been found to be up-regulated in most biopsies obtained from recurrent NSCLC patients showing signs of EMT in response to the induction of erlotinib resistance[65]. In accordance with our other findings, we found that *N-cadherin* was significantly decreased in the PC-9/Erl-Rd xenograft tissues following treatment with silibinin.

Silibinin reverses the mesenchymal phenotype of erlotinib-refractory PC-9/Erl-R cells *in vitro*. To confirm that the effects observed with regard to EMT-related erlotinib efficacy in the mice treated with oral silibinin were also due to the direct effect of silibinin on the tumor cells, and not only on the mouse tissue micro-environment, we evaluated whether silibinin alone was sufficient to reactivate an epithelial phenotype in erlotinib-refractory PC-9/Erl-R mesenchymal cells *in vitro*. Microscopically, the PC-9/Erl-R cells exhibited a spindle cell-like morphology that was notably different from the parental PC-9 cells. As expected, the erlotinib-refractory PC-9/Erl-R cells displayed EMT features, including the reorganization of filamentous actin (F-actin), with a significant enhancement of stress fibers, a decrease in the abundance of the epithelial cell-cell adhesion protein, E-cadherin, and an increase in the abundance of the mesenchymal adhesion protein vimentin when compared to the erlotinib-responsive PC-9 parental epithelial cells (**Figs. 4 and 5**). Of note, treatment with silibinin-meglumine induced the re-expression of E-cadherin, which correlated with morphological changes consistent with the erlotinib-refractory PC-9/Erl-R cells undergoing the reciprocal mesenchymal-to-epithelial transition (MET). Analyses of the actin stress fibers and vimentin expression before and after treatment with silibinin-meglumine revealed that the PC-9/Erl-R cells had reverted from the erlotinib-refractory, acquired mesenchymal state to the original, erlotinib-sensitive, *de novo* epithelial cellular state (**Figs. 4 and 5**). Importantly, all these phenomena related to changes in the cell migratory behavior of PC-9/Erl-R cells. *In vitro* scratch wound healing assays showed that the highly migratogenic phenotype of PC-9/Erl-R cells was largely prevented in the presence of silibinin; thus, silibinin-treated PC-9/Erl-R cells demonstrated a significantly slower cell migration speed compared to the basal locomotory activity of untreated PC-9/ErlR cells (**Fig. 5**).

Discussion

By culturing erlotinib-hypersensitive PC-9 cells harboring the erlotinib-sensitizing *EGFR* exon 19 mutation *ΔE746-A750* in the presence of high concentrations of erlotinib over a period of several months, we were able to isolate PC-9 derivatives capable of growing at erlotinib concentrations of up to 10 μmol/L[34]. We recently described that, in the absence of second-site *EGFR* mutations, alternative activation of MET, AXL, or HER2, gain of secondary mutations in the *KRAS*, *NRAS*, or *BRAF* genes, and loss of the mutant *delE746-A750 EGFR* gene itself[66], acquired resistance to erlotinib is mostly correlated with a significant enrichment in EMT features[34]. By taking advantage of this unique model of non-mutational, EMT-driven acquired resistance to erlotinib, we explored whether an oral formulation of a milk thistle extract enriched (30% *w/w*) with a water-soluble derivative of the bioactive lignan silibinin (*i.e.,* silibinin complexed with the excipient amino-sugar meglumine) was able to circumvent erlotinib resistance in EGFR-mutant PC-9/Erl-R xenografts. This paper reports, for the first time, the inhibitory effect of silibinin on NSCLC cancer growth in an *in vivo* xenograft model of EMT-driven acquired resistance to erlotinib that was generated by the subcutaneous injection of PC-9/Erl-R cells in athymic mice. Specifically, we demonstrated that 5 weeks of oral administration of 100 mg/kg per day silibinin was sufficient to significantly inhibit the growth of PC-9/Erl-R tumor xenografts, Importantly, our data demonstrate that silibinin can reverse the resistance to erlotinib because mice concurrently exposed to silibinin and erlotinib show an impressive 85% reduction in tumor growth after 35 days of combined treatment. No evidence of tumor regrowth was noted in the combination group, even after discontinuation of the drugs for two weeks. Although these findings suggest that the biological activity of silibinin might continue after administration has ceased, long-term monitoring of tumor growth and spread in the mice should be performed before unambiguously concluding that silibinin improves recurrence free survival in our erlotinib-refractory xenograft models.
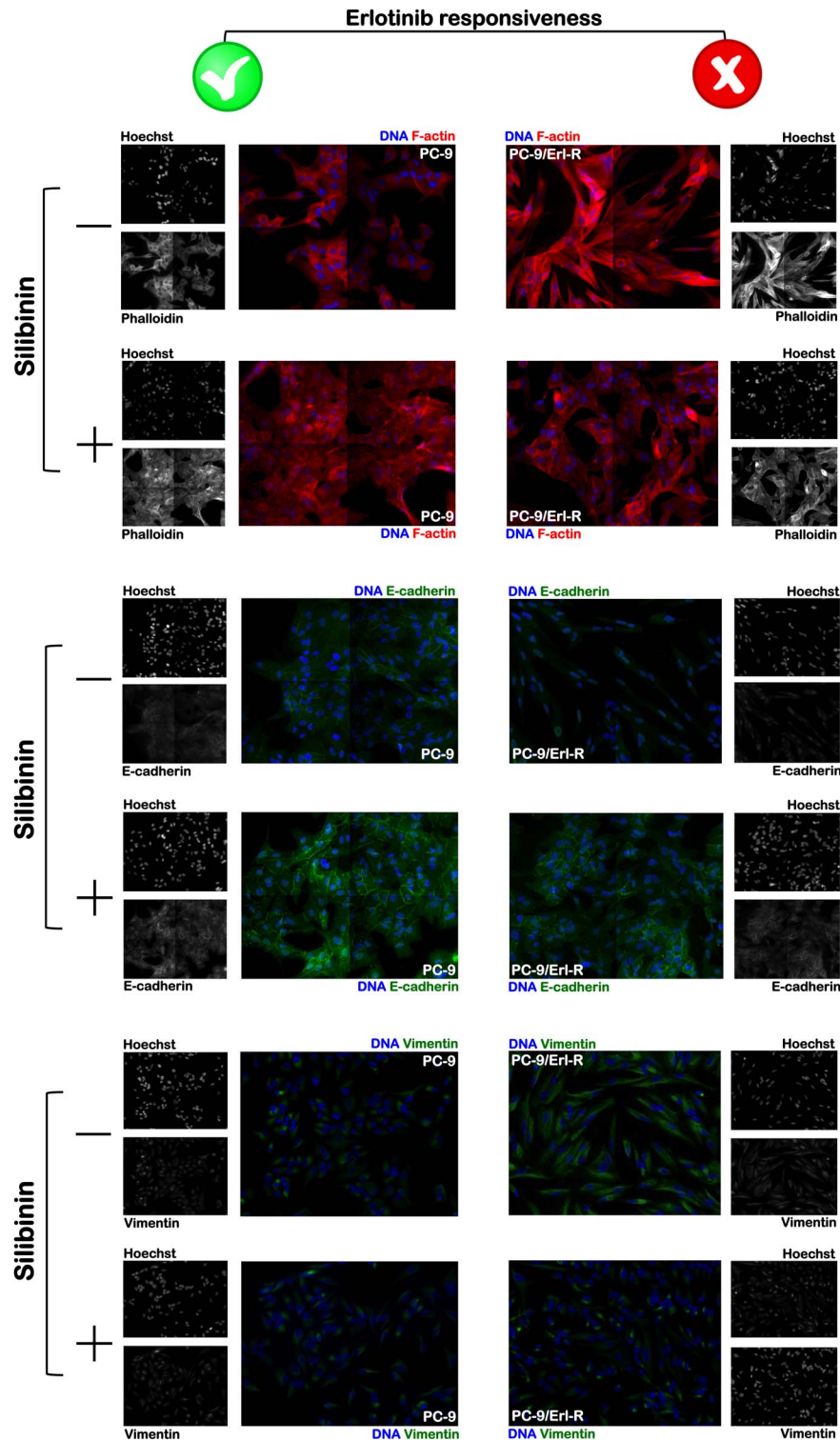
Figure 4 | **Silibinin enhances the epithelial phenotype in PC-9 parental cells and reverses the mesenchymal phenotype in PC-9/Erl-R cells (I).** PC-9 parental cells and erlotinib-resistant PC-9/Erl-R cells were cultured for 3 days in the absence or presence of 100 μg/mL of silibinin-meglumine. *Top panels.* After fixation and permeabilization, the subcellular distribution of F-actin, the epithelial marker E-cadherin, and of the mesenchymal-specific marker vimentin was assessed after staining with anti-F-actin, anti-E-cadherin, and anti-vimentin antibodies and Hoechst 33258 for nuclear counterstaining, as specified. Images show representative portions of the untreated- and silibinin meglumine-treated cells in montages of 4 × 4, which were captured in different channels for F-actin (*red*), E-cadherin (*green*), vimentin (*green*), and Hoechst 33258 (*blue*) with a 20× objective. Images were merged on a BD Pathway 855 Bioimager System with BD Attovision software.

The process of EMT is regulated by the expression status of specific miRNAs during tumor development and disease progression; *miR-21* is one such miRNA that is overexpressed in solid tumors compared to paired benign and normal tissues. Indeed, *miR-21* is considered to be an oncogenic miRNA that exhibits anti-apoptotic activity in various types of cancer cells and appears to control the EMT process and the CSC phenotype by targeting PTEN or collaborating with the EMT transcription factor *SNAIL*[51–56]. This suggests
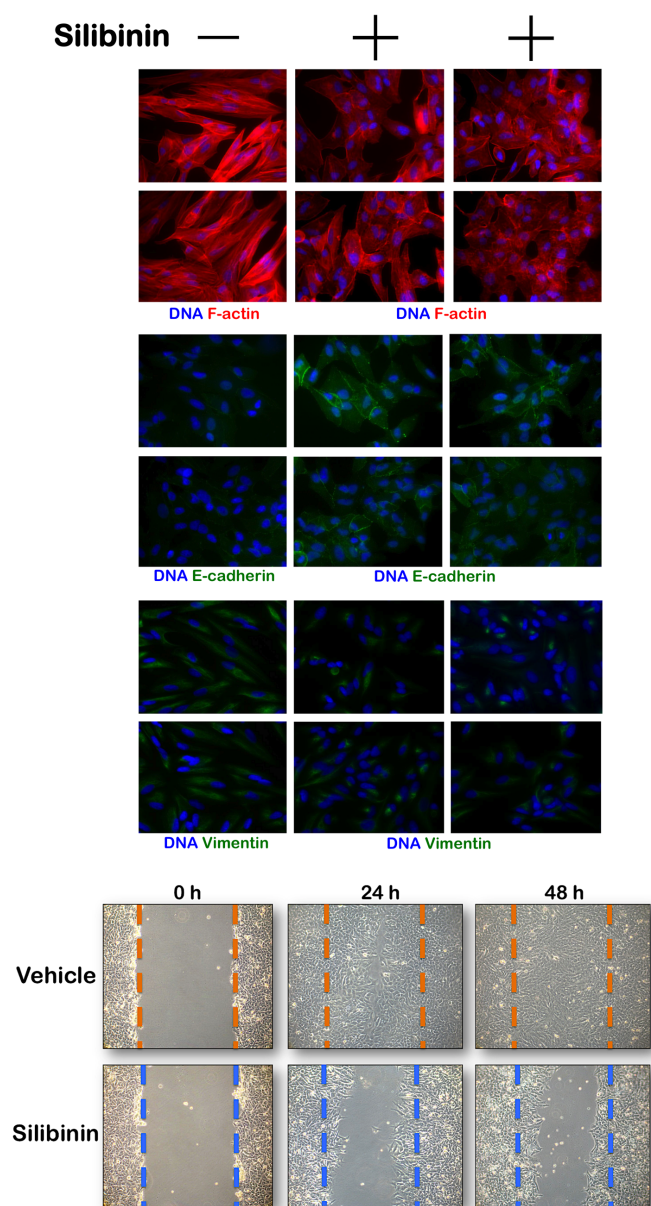
Figure 5 | Silibinin promotes mesenchymal to epithelial conversion of erlotinib-resistant PC-9/Erl-R cells. *Top panels.* Erlotinib-resistant PC-9/Erl-R cells were cultured for 3 days in the absence or presence of 100 µg/mL of silibinin. *Top panels.* After fixation and permeabilization, the subcellular distribution of F-actin, the epithelial marker E-cadherin, and of the mesenchymal-specific marker vimentin was assessed after staining with anti-F-actin, anti-E-cadherin, and anti-vimentin antibodies and Hoechst 33258 for nuclear counterstaining, as specified. Images show representative portions of the untreated- and silibinin meglumine-treated cells, which were captured in different channels for F-actin (*red*), E-cadherin (*green*), vimentin (*green*), and Hoechst 33258 (*blue*) with a 20× objective. Images were merged on a BD Pathway 855 Bioimager System with BD Attovision software. *Bottom panels.* Figure shows representative microphotographs of wound healing assays 0, 24, and 48 h after incisions of confluent PC-9/ErL-R cells cultured in the absence or presence of silibinin (100 µg/mL).

that the antagonism of *miR-21* could be therapeutically beneficial for the treatment of drug-refractory tumors that are driven by EMT-like phenomena. The *miR-200* family is another example of a group of miRNAs associated with cancer recurrence and overall survival that plays an important role in the regulation of EMT. The low expression of members of the *miR-200* family plays an important role in cancer

metastasis by controlling the EMT process and EMT-driven resistance to cancer therapies[37,41,60–64,67–69]. The reactivation of *miR-200* by novel approaches may serve as an inhibitor of EMT, which may either reverse or eliminate the EMT phenotype, enabling anti-cancer drugs, such as EGFR-directed therapy, to effectively circumvent EMT-associated drug resistance. In this study, we first compared the expression of EMT-related miRNAs between erlotinib-sensitive and erlotinib-refractory NSCLC tumor tissues and investigated whether the natural agent silibinin could function as a novel microRNA-modulating anticancer agent. We found that the expression levels of *miR-21* and *miR-200c* were significantly up-regulated and down-regulated, respectively, in the erlotinib-refractory tumors. Accordingly, these tumors showed EMT characteristics, including a high expression of such mesenchymal markers as *SNAIL*, *ZEB*, and *N-cadherin*. Interestingly, we also documented that the increased expression of *miR-21* and attenuated expression of *miR-200c*, a signature of tumor aggressiveness, in the erlotinib-resistant tumors was significantly affected by treatment with silibinin. Indeed, silibinin treatment down-regulated *miR-21* and up-regulated *miR-200c*, and, consequently, the reversion of the high *miR-21*/low *miR-200c* signature resulted in the down-regulation of *SLUG*, *ZEB1*, and *N-cadherin*, a result that was consistent with the reversal of the EMT phenotype. We also showed that the combination of silibinin with erlotinib was much more effective than either agent alone, suggesting that the alterations in specific miRNAs mediated by silibinin, which led to the reversal of the mesenchymal phenotype, could be a novel approach for the prevention of erlotinib resistance in NSCLC treatment. Nevertheless, it is reasonable to suggest that silibinin should be added to the current list of microRNA-modulating anticancer agents that can efficiently target the EMT phenotype.

Our results should prompt further interest in the use of silibinin as a drug modality, as they raise the possibility that the EMT arising during erlotinib-resistance development, as observed in EGFR-mutant NSCLC, can be countered by the silibinin combination. This can be readily tested in a clinical setting; indeed, there has been an effort to translate the relevance of preclinical anticancer efficacy studies into the clinical setting, specifically with regard to determining the comparable doses required for humans. In this respect, the calculation of the human equivalent dose (HED) using normalization of the body surface area rather than weight has been advocated[70]. On the basis of the formula proposed for calculating HED, animal dose (mg/kg) x (animal *Km factor*/human *Km factor*), we found that the corresponding HED for the maximum dose of silibinin used in our *in vivo* study, which was equivalent to 100 mg/kg mouse body weight, is a human equivalent dose of 8.11 mg/kg. This equates to a 486.49-mg dose of silibinin for a 60-kg individual, an HED that is likely within the dose that can be achieved in target cancer tissues. When colorectal cancer patients were given 1.45 g/day of silipide, a formulation of silibinin with better bioavailability, for 7 days, this dosage was found to be safe and achieved levels of up to 4 µmol/L in the plasma, 2.5 nmol/g tissue in the liver, and 141 nmol/g in the colorectal tissue[71]. Thus, the effective doses of silibinin used in the present *in vivo* study are within the range of physiologically achievable concentrations of silibinin found in the tissues of cancer patients given similar doses of silibinin. Moreover, it is known that silibinin has poor water solubility. However, the ionization ability of silibinin increases when it is combined with meglumine, and silibinin-meglumine has a high water solubility. Our development of a water-soluble formulation of silibinin is crucial for target preparations, as it will enable new formulation breakthroughs for silibinin-meglumine-containing injections, granules, or beverages. In addition, one of the principles of combination therapy is that the side effects of the two drugs should not overlap. Considering the relatively non-toxic nature of such natural agents as silibinin, which has been widely used for many years with negligible toxicity, better treatment outcomes may be achieved through the novel and safe approach of targeting EMT-type,
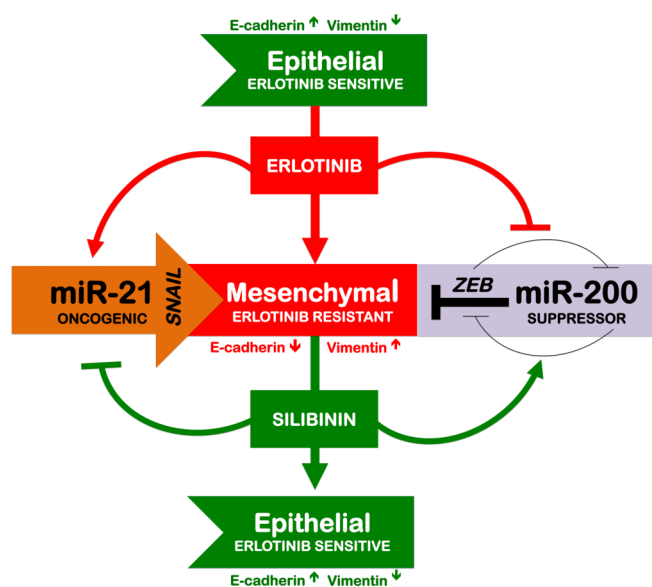
Figure 6 | Water-soluble silibinin: A new strategy for targeted *in vivo* control of molecules that regulate the acquisition of an EGFR TKI-refractory mesenchymal-like phenotype in EGFR mutant-NSCLC cells.

erlotinib-refractory NSCLC cells with silibinin-meglumine combined with EGFR TKIs (such as erlotinib). A highly efficacious, long-term drug-release delivery system for silibinin-meglumine that must be safe after oral or intravenous administration needs to be developed. The pre-clinical findings of the present study, along with the lack of any apparent toxicity associated with silibinin, underscore the efficacy of silibinin against erlotinib-refractory, EGFR-mutant NSCLC, with translational potential in the immediate future.

Because mesenchymal-type NSCLC cancer cells are more resistant to EGFR TKIs than epithelial-type NSCLC cancer cells, regardless of the EGFR mutation status, and given that various erlotinib-resistance mechanisms occur *via* the induction of EMT, the discovery of pharmacological approaches that are able to reverse the tumor status of EMT features could identify new strategies for sensitizing this important subgroup of EGFR TKI-resistant NSCLC tumors. The results presented in this article showed, for the first time, that the nontoxic, natural agent silibinin can effectively reverse EMT. Specifically, silibinin activates the MET genetic program in EGFR-mutant NSCLC cells that have acquired resistance to erlotinib. Mechanistically, this phenotype is associated with the EMT-related high *miR-21*/low *miR-200c* microRNA signature (**Fig. 6**). We also found that silibinin down-regulates the expression of *miR-21* and promotes the re-expression of *miR-200c* in erlotinib-refractory tumors, providing a molecular mechanism for the observed reversal of EMT to MET, along with the complete reversal of erlotinib resistance *in vivo*. These novel findings suggest that the anticancer activity of the bioactive lignan silibinin against aggressive NSCLC tumors is, in part, due to the reversal of the EMT phenotype. The administration of a water-soluble, silibinin-rich milk thistle extract should be tested in upcoming clinical trials to assess whether it can prevent or reverse EMT-driven NSCLC progression following erlotinib treatment.

Methods

Drugs and chemicals. The water-soluble milk thistle extract was provided by Monteloeder, S. L. in its silibinin-meglumine salt form (Elche, Alicante, Spain). The milk thistle extract composition was analyzed and quantified by HPLC–145 DAD-ESI-MS/MS on an Agilent LC 1100 series (Agilent Technologies, Inc., Palo Alto, CA, USA). The retention time, UV spectra, and MS/MS data of the sample peaks were compared to data reported in the literature[72–74]. Quantitation of the main flavonolignan compounds was performed using ChemStation for LC 3D software (Agilent Technologies Life Sciences and Chemical Analysis, Waldbronn, Germany),

and the silibinin equivalents were determined with silibinin standards (Sigma–Aldrich). The EGFR (HER1) TKI erlotinib (Tarceva®) was a kind gift from Roche Pharmaceuticals. Stock solutions of erlotinib at 10 mmol/L were prepared in DMSO, and aliquots were stored in the dark at −20°C until use. For the experiments, all drug solutions were prepared fresh from stock solutions and were diluted with the cell growth medium. The control cells were cultured in media containing identical concentrations (*v/v*) of vehicle.

Generation of PC-9 cells with acquired resistance to erlotinib. PC-9 NSCLC-derived cells expressing the EGFR exon 19 deletion mutation (*delE746-A750*) were obtained from the IBL cell bank (Gunma, Japan). PC-9 cells with acquired resistance to erlotinib were generated as previously described[34].

Tumor cell implantation experiments. A total of 40 female athymic nude mice (four to five weeks old, 23 to 25 g) purchased from Harlam Laboratories (France) were subcutaneously inoculated with $5 \times 10^6/100$ µl PC-9/Erl-R cells. Two independent experiments were performed, and the data obtained from the two experiments were pooled. Subcutaneous tumor growth was monitored daily; when the solid tumors reached a volume of 100 mm³, the animals were randomly assigned to groups of 6 animals each. These groups were treated with vehicle control, erlotinib (100 mg/kg, 5 days a week), silibinin-meglumine (100 mg/kg, 5 days a week), or erlotinib plus silibinin-meglumine. All the drugs were administered *via* oral gavage. The mice were weighed once per week after dosing, the tumor sizes were measured daily with electronic calipers, and the tumor volumes were calculated with the following formula: volume (mm³) = length × width2 × 0.5. The experiments were approved by the Institutional Animal Care and Use Committee (IACUC) of the Institut d'Investigació Biomèdica de Bellvitge (IDIBELL; Animal Use Protocol #6302 authorized by the Animal Experimental Commission of the Catalan Government, Barcelona, Spain). After 35 days of oral treatment, the mice were killed by cervical dislocation, and the tumors were collected. The tumor samples were divided for DNA, microRNA, and mRNA analyses.

Quantitative real-time polymerase chain reaction (qRT-PCR). For the purification of microRNA and total RNA from the tumor tissues, we used Qiagen miRNeasy Mini kits (Cat. No. 217004) and QIAshredder columns, according to the manufacturer's instructions. To complete the miRNA PCR assay procedure, we reverse transcribed our small RNA samples into first-strand cDNA, the template for PCR, using the RT² miRNA First Strand Kit (Cat. No. MA-03/331401; SABiosciences). Real-time PCR-based miRNA expression profiling was performed with a customized miRNA PCR array in a 96-well format, as described in the SABiosciences RT miRNA qPCR Assays manual. One microgram of total RNA was reverse-transcribed to cDNA using the Reaction Ready™ First Strand cDNA Synthesis Kit (SABiosciences) and applied to a customized PCR array in a 96-well format. The PCR array contained the following panel of genes: *GSC, KRT14, KRT19, NUMB, TCF3, TCF4, SDC1, ZO-1, CD44, TWIST, SNAI1, VIM, SLUG, CDH1, ZEB1, CDH2, ZEB2, FN1,* and *CD24*. The arrays were processed according to the SABiosciences RT-PCR manual and analyzed using an Applied Biosystems 7500 Fast Real-Time PCR System with an automated baseline and threshold cycle detection. The data were interpreted using a web-based PCR array analysis tool from SABiosciences.

Immunofluorescence staining and high-content confocal imaging. For imaging, the cells were seeded at a density of approximately 5,000 cells/well in 96-well clear-bottom tissue culture plates (Becton Dickinson Biosciences; San Jose, CA) optimized for automated imaging applications. Triton® X-100 permeabilization and blocking, primary antibody staining, secondary antibody staining using Alexa Fluor® 488/594 goat anti-rabbit/mouse IgGs (Invitrogen-Molecular Probes, Eugene, Oregon), and counterstaining (using Hoechst 33258; Invitrogen) were performed according to protocols from BD Biosciences. The images were captured in different channels for Alexa Fluor® 488 (pseudocolored green), Alexa Fluor® 594 (pseudocolored red), and Hoechst 33258 (pseudocolored blue) using a BD Pathway™ 855 Bioimager System (Becton Dickinson Biosciences, San Jose, California) with 20× or 40× objectives (NA 075 Olympus). Merged images were obtained according to the recommended Assay Procedure using the BD Attovision™ software.

Wound-healing motility assays. PC-9/Erl-R cells were seeded onto six-well dishes at 1×10^5 per well. A single scratch wound was creased using a p10 micropipette tip into confluent cells. Cells were washed twice with PBS to remove cell debris, supplemented with regular growth medium in the absence or presence of silibinin, and monitored. Images were captured by phase-contrast microscopy at 0, 24, and 48 h after wounding.

1. Rosell, R. *et al.* Screening for epidermal growth factor receptor mutations in lung cancer. *N Engl J Med.* **361**, 958–67 (2009).
2. Rosell, R. *et al.* Predictive biomarkers in the management of EGFR mutant lung cancer. *Ann N Y Acad Sci* **1210**, 45–52 (2010).
3. Rosell, R. *et al.* Non-small-cell lung cancer harbouring mutations in the EGFR kinase domain. *Clin Transl Oncol* **12**, 75–80 (2010).
4. Rosell, R. *et al.* Erlotinib versus standard chemotherapy as first-line treatment for European patients with advanced EGFR mutation-positive non-small-cell lung cancer (EURTAC): a multicentre, open-label, randomised phase 3 trial. *Lancet Oncol* **13**, 239–46 (2012).

5. Santarpia, M., De Pas, T. M., Altavilla, G., Spaggiari, L. & Rosell, R. Moving towards molecular-guided treatments: erlotinib and clinical outcomes in non-small-cell lung cancer patients. *Future Oncol* **9**, 327–45 (2013).
6. Morgillo, F., Bareschino, M. A., Bianco, R., Tortora, G. & Ciardiello, F. Primary and acquired resistance to anti-EGFR targeted drugs in cancer therapy. *Differentiation* **75**, 788–99 (2007).
7. Nguyen, K. S., Kobayashi, S. & Costa, D. B. Acquired resistance to epidermal growth factor receptor tyrosine kinase inhibitors in non-small-cell lung cancers dependent on the epidermal growth factor receptor pathway. *Clin Lung Cancer* **10**, 281–9 (2009).
8. Gazdar, A. F. Activating and resistance mutations of EGFR in non-small-cell lung cancer: role in clinical response to EGFR tyrosine kinase inhibitors. *Oncogene* **28 Suppl 1**, S24–S31 (2009).
9. Xu, Y., Liu, H., Chen, J. & Zhou, Q. Acquired resistance of lung adenocarcinoma to EGFR-tyrosine kinase inhibitors gefitinib and erlotinib. *Cancer Biol Ther* **9**, 572–82 (2010).
10. Ayoola, A., Barochia, A., Belani, K. & Belani, C. P. Primary and acquired resistance to epidermal growth factor receptor tyrosine kinase inhibitors in non-small cell lung cancer: an update. *Cancer Invest* **30**, 433–46 (2012).
11. Lin, L. & Bivona, T. G. Mechanisms of Resistance to Epidermal Growth Factor Receptor Inhibitors and Novel Therapeutic Strategies to Overcome Resistance to NSCLC Patients. *Chemother Res Pract* **2012**, 817297 (2012).
12. Nakata, A. & Gotoh, N. Recent understanding of the molecular mechanisms for the efficacy and resistance of EGF receptor-specific tyrosine kinase inhibitors in non-small cell lung cancer. *Expert Opin Ther Targets* **16**, 771–81 (2012).
13. Sequist, L. V. et al. Genotypic and histological evolution of lung cancers acquiring resistance to EGFR inhibitors. *Sci Transl Med* **3**, 75ra26 (2011).
14. Thomson, S. et al. Epithelial to mesenchymal transition is a determinant of sensitivity of non-small-cell lung carcinoma cell lines and xenografts to epidermal growth factor receptor inhibition. *Cancer Res* **65**, 9455–62 (2005).
15. Fuchs, B. C. et al. Epithelial-to-mesenchymal transition and integrin-linked kinase mediate sensitivity to epidermal growth factor receptor inhibition in human hepatoma cells. *Cancer Res* **68**, 2391–9 (2008).
16. Yauch, R. L. et al. Epithelial versus mesenchymal phenotype determines in vitro sensitivity and predicts clinical activity of erlotinib in lung cancer patients. *Clin Cancer Res* **11**, 8686–98 (2005).
17. Coldren, C. D. et al. Baseline gene expression predicts sensitivity to gefitinib in non-small cell lung cancer cell lines. *Mol Cancer Res* **4**, 521–528 (2006).
18. Suda, K. et al. Epithelial to mesenchymal transition in an epidermal growth factor receptor-mutant lung cancer cell line with acquired resistance to erlotinib. *J Thorac Oncol* **6**, 1152–61 (2011).
19. Chung, J. H. et al. Clinical and molecular evidences of epithelial to mesenchymal transition in acquired resistance to EGFR-TKIs. *Lung Cancer* **73**, 176–82 (2011).
20. Chang, T. H. et al. Slug confers resistance to the epidermal growth factor receptor tyrosine kinase inhibitor. *Am J Respir Crit Care Med* **183**, 1071–9 (2011).
21. Bryant, J. L. et al. A microRNA gene expression signature predicts response to erlotinib in epithelial cancer cell lines and targets EMT. *Br J Cancer* **106**, 148–56 (2012).
22. Zhang, X. et al. N-Cadherin Expression Is Associated with Acquisition of EMT Phenotype and with Enhanced Invasion in Erlotinib-Resistant Lung Cancer Cell Lines. *PLoS One* **8**, e57692 (2013).
23. Zhang, Z. et al. Activation of the AXL kinase causes resistance to EGFR-targeted therapy in lung cancer. *Nat Genet* **44**, 852–60 (2012).
24. Byers, L. A. et al. An epithelial-mesenchymal transition (EMT) gene signature predicts resistance to EGFR and PI3K inhibitors and identifies Axl as a therapeutic target for overcoming EGFR inhibitor resistance. *Clin Cancer Res* **19**, 279–90 (2013).
25. Nurwidya, F., Takahashi, F., Murakami, A. & Takahashi, K. Epithelial mesenchymal transition in drug resistance and metastasis of lung cancer. *Cancer Res Treat* **44**, 151–6 (2012).
26. Post-White, J., Ladas, E. J. & Kelly, K. M. Advances in the use of milk thistle (Silybum marianum). *Integr Cancer Ther* **6**, 104–9 (2007).
27. Gazák, R., Walterová, D. & Kren, V. Silybin and silymarin–new and emerging applications in medicine. *Curr Med Chem* **14**, 315–38 (2007).
28. Agarwal, R., Agarwal, C., Ichikawa, H., Singh, R. P. & Agarwal, B. B. Anticancer potential of silymarin: from bench to bed side. *Anticancer Res* **26**, 4457–98 (2006).
29. Singh, R. P. & Agarwal, R. Prostate cancer chemoprevention by silibinin: bench to bedside. *Mol Carcinog* **45**, 436–42 (2006).
30. Rho, J. K. et al. Combined treatment with silibinin and epidermal growth factor receptor tyrosine kinase inhibitors overcomes drug resistance caused by T790M mutation. *Mol Cancer Ther* **9**, 3233–43 (2010).
31. Singh, R. P., Raina, K., Sharma, G. & Agarwal, R. Silibinin inhibits established prostate tumor growth, progression, invasion, and metastasis and suppresses tumor angiogenesis and epithelial-mesenchymal transition in transgenic adenocarcinoma of the mouse prostate model mice. *Clin Cancer Res* **14**, 7773–80 (2008).
32. Wu, K. et al. Silibinin reverses epithelial-to-mesenchymal transition in metastatic prostate cancer cells by targeting transcription factors. *Oncol Rep* **23**, 1545–52 (2010).
33. Deep, G., Gangar, S. C., Agarwal, C. & Agarwal, R. Role of E-cadherin in antimigratory and antiinvasive efficacy of silibinin in prostate cancer cells. *Cancer Prev Res (Phila)* **4**, 1222–32 (2011).
34. Cufí, S. et al. IGF-1R/epithelial-to-mesenchymal transition (EMT) crosstalk suppresses the erlotinib-sensitizing effecy of EGFR exon 19 deletion mutations. *Sci. Rep.* In press.
35. Wright, J. A., Richer, J. K. & Goodall, G. J. microRNAs and EMT in mammary cells and breast cancer. *J Mammary Gland Biol Neoplasia* **15**, 213–23 (2010).
36. Wang, Z. et al. Targeting miRNAs involved in cancer stem cell and EMT regulation: An emerging concept in overcoming drug resistance. *Drug Resist Updat* **13**, 109–18 (2010).
37. Brabletz, S. & Brabletz, T. The ZEB/miR-200 feedback loop--a motor of cellular plasticity in development and cancer? *EMBO Rep* **11**, 670–7 (2010).
38. Zhang, J. & Ma, L. MicroRNA control of epithelial-mesenchymal transition and metastasis. *Cancer Metastasis Rev* **31**, 653–62 (2012).
39. Bullock, M. D., Sayan, A. E., Packham, G. K. & Mirnezami, A. H. MicroRNAs: critical regulators of epithelial to mesenchymal (EMT) and mesenchymal to epithelial transition (MET) in cancer progression. *Biol Cell* **104**, 3–12 (2012).
40. Hill, L., Browne, G. & Tulchinsky, E. ZEB/miR-200 feedback loop: at the crossroads of signal transduction in cancer. *Int J Cancer* **132**, 745–54 (2013).
41. Li, Y. et al. Up-regulation of miR-200 and let-7 by natural agents leads to the reversal of epithelial-to-mesenchymal transition in gemcitabine-resistant pancreatic cancer cells. *Cancer Res* **69**, 6704–12 (2009).
42. Li, Y., Kong, D., Wang, Z. & Sarkar, F. H. Regulation of microRNAs by natural agents: an emerging field in chemoprevention and chemotherapy research. *Pharm Res* **27**, 1027–41 (2010).
43. Sarkar, F. H., Li, Y., Wang, Z., Kong, D. & Ali, S. Implication of microRNAs in drug resistance for designing novel cancer therapy. *Drug Resist Updat* **13**, 57–66 (2010).
44. Wang, Z. et al. Targeting miRNAs involved in cancer stem cell and EMT regulation: An emerging concept in overcoming drug resistance. *Drug Resist Updat* **13**, 109–18 (2010).
45. Ali, S. et al. Gemcitabine sensitivity can be induced in pancreatic cancer cells through modulation of miR-200 and miR-21 expression by curcumin or its analogue CDF. *Cancer Res* **70**, 3606–17 (2010).
46. Mukhopadhyay, P. et al. Restoration of altered microRNA expression in the ischemic heart with resveratrol. *PLoS One* **5**, e15705 (2010).
47. Fix, L. N., Shah, M., Efferth, T., Farwell, M. A. & Zhang, B. MicroRNA expression profile of MCF-7 human breast cancer cells and the effect of green tea polyphenon-60. *Cancer Genomics Proteomics* **7**, 261–77 (2010).
48. Sheth, S. et al. Resveratrol reduces prostate cancer growth and metastasis by inhibiting the Akt/MicroRNA-21 pathway. *PLoS One* **7**, e51655 (2012).
49. Shah, M. S., Davidson, L. A. & Chapkin, R. S. Mechanistic insights into the role of microRNAs in cancer: influence of nutrient crosstalk. *Front Genet* **3**, 305 (2012).
50. Yu, Y., Sarkar, F. H. & Majumdar, A. P. Down-regulation of miR-21 Induces Differentiation of Chemoresistant Colon Cancer Cells and Enhances Susceptibility to Therapeutic Regimens. *Transl Oncol* **6**, 180–6 (2013).
51. Cottonham, C. L., Kaneko, S. & Xu, L. miR-21 and miR-31 converge on TIAM1 to regulate migration and invasion of colon carcinoma cells. *J Biol Chem* **285**, 35293–302 (2010).
52. Bao, B. et al. Notch-1 induces epithelial-mesenchymal transition consistent with cancer stem cell phenotype in pancreatic cancer cells. *Cancer Lett* **307**, 26–36 (2011).
53. Han, M. et al. Re-expression of miR-21 contributes to migration and invasion by inducing epithelial-mesenchymal transition consistent with cancer stem cell characteristics in MCF-7 cells. *Mol Cell Biochem* **363**, 427–36 (2012).
54. Han, M. et al. MiR-21 regulates epithelial-mesenchymal transition phenotype and hypoxia-inducible factor-1α expression in third-sphere forming breast cancer stem cell-like cells. *Cancer Sci* **103**, 1058–1064 (2012).
55. Bornachea, O. et al. EMT and induction of miR-21 mediate metastasis development in Trp53-deficient tumours. *Sci Rep* **2**, 434 (2012).
56. Han, M. et al. Antagonism of miR-21 reverses epithelial-mesenchymal transition and cancer stem cell phenotype through AKT/ERK1/2 inactivation by targeting PTEN. *PLoS One* **7**, e39520 (2012).
57. Liu, X. et al. MicroRNA-31 functions as an oncogenic microRNA in mouse and human lung cancer cells by repressing specific tumor suppressors. *J Clin Invest* **120**, 1298–309 (2010).
58. Tan, X. et al. A 5-microRNA signature for lung squamous cell carcinoma diagnosis and hsa-miR-31 for prognosis. *Clin Cancer Res* **17**, 6802–11 (2011).
59. Hua, S. et al. Reduced miR-31 and let-7 maintain the balance between differentiation and quiescence in lung cancer stem-like side population cells. *Biomed Pharmacother* **66**, 89–97 (2012).
60. Burk, U. et al. A reciprocal repression between ZEB1 and members of the miR-200 family promotes EMT and invasion in cancer cells. *EMBO Rep* **9**, 582–589 (2008).
61. Adam, L. et al. miR-200 expression regulates epithelial-to-mesenchymal transition in bladder cancer cells and reverses resistance to epidermal growth factor receptor therapy. *Clin Cancer Res* **15**, 5060–72 (2009).
62. Tryndyak, V. P., Beland, F. A. & Pogribny, I. P. E-cadherin transcriptional down-regulation by epigenetic and microRNA-200 family alterations is related to mesenchymal and drug-resistant phenotypes in human breast cancer cells. *Int J Cancer* **126**, 2575–83 (2010).
63. Wellner, U. et al. The EMT-activator ZEB1 promotes tumorigenicity by repressing stemness-inhibiting microRNAs. *Nat Cell Biol* **11**, 1487–95 (2009).
64. Lim, Y. et al. Epigenetic modulation of the miR-200 family is associated with transition to a breast cancer stem cell-like state. *J Cell Sci* **126**, 2256–66 (2013).

65. Zhang, X. *et al*. N-cadherin expression is associated with acquisition of EMT phenotype and with enhanced invasion in erlotinib-resistant lung cancer cell lines. *PLoS One* **8**, e57692 (2013).

66. Tabara, K. *et al*. Loss of activating EGFR mutant gene contributes to acquired resistance to EGFR tyrosine kinase inhibitors in lung cancer cells. *PLoS One* **7**, e41017 (2012).

67. Olson, P. *et al*. MicroRNA dynamics in the stages of tumorigenesis correlate with hallmark capabilities of cancer. *Genes Dev* **23**, 2152–65 (2009).

68. Manavalan, T. T. *et al*. Reduced Expression of miR-200 Family Members Contributes to Antiestrogen Resistance in LY2 Human Breast Cancer Cells. *PLoS One* **8**, e62334 (2013).

69. Radisky, D. C. miR-200c at the nexus of epithelial-mesenchymal transition, resistance to apoptosis, and the breast cancer stem cell phenotype. *Breast Cancer Res* **13**, 110 (2011).

70. Reagan-Shaw, S., Nihal, M. & Ahmad, N. Dose translation from animal to human studies revisited. *FASEB J* **22**, 659–61 (2008).

71. Hoh, C. *et al*. Pilot study of oral silibinin, a putative chemopreventive agent, in colorectal cancer patients: silibinin levels in plasma, colorectum, and liver and their pharmacodynamic consequences. *Clin Cancer Res* **12**, 2944–50 (2006).

72. Brinda, B. J., Zhu, H. J. & Markowitz, J. S. A sensitive LC-MS/MS assay for the simultaneous analysis of the major active components of silymarin in human plasma. *J Chromatogr B Analyt Technol Biomed Life Sci* **902**, 1–9 (2012).

73. Kuki, A. *et al*. Identification of silymarin constituents: An improved HPLC-MS method. *Chromatographia* **75**, 175–80 (2012).

74. Wang, K., Zhang, H., Shen, L., Du, Q. & Li, J. Rapid separation and characterization of active flavonolignans of Silybum marianum by ultra-performance liquid chromatography coupled with electrospray tandem mass spectrometry. *J Pharm Biomed Anal* **53**, 1053–7 (2010).

Acknowledgements

Author contributions

J.A.M., J.B.-B., A.S.-C., J.J., V.M. and A.V.M. designed the study. S.C., C.O.F., A.V.M., V.Z.T.-G., J.J., E.C., B.C.F., R.B., A.S.-C., E.B.-C. and E.C. performed the experiments. J.A.M., V.M., B.M.C., J.B.-B., J.J. and J.V. analysed the data. J.A.M. wrote the paper.

Additional information

Supplementary information accompanies this paper at http://www.nature.com/scientificreports

Competing financial interests: AstraZeneca (Spain) provided partial financial support for the present study via an educational grant to Dr. Javier A. Menendez and Dr. Joaquim Bosch-Barrera.

How to cite this article: Cufí, S. *et al*. Silibinin suppresses EMT-driven erlotinib resistance by reversing the high *miR-21*/low *miR-200c* signature *in vivo*. *Sci. Rep*. **3**, 2459; DOI:10.1038/srep02459 (2013).